ARTICLE

Fabrication of Melamine/Tb³⁺-Intercalated Polydiacetylene Nanosheets and Their Thermochromic Reversibility

Qing Wang, Gang Wang, Xia-yun Huang*, Dao-yong Chen*

State Key Laboratory of Molecular Engineering of Polymers, Department of Macromolecular Science, Fudan University, Shanghai 200438, China

Polydiacetylene (PDA) is one kind of the conjugated polymer with layered structure, which can serve as a host to accommodate the guest components through intercalation. In these intercalated PDAs, some of them were reported to have a nearly perfect organized structure and perform completely reversible thermochromism. Till now, these reported intercalated PDAs were made by only introducing a single component for intercalation. Here, we chose 10,12-pentacosadiynoic acid (PCDA) as the monomer, of which the carboxyl-terminal groups can interact with either Tb^{3+} ions or melamines (MAs). When the feeding molar ratio of PCDA, MA, and Tb^{3+} ion was 3:267:1, only Tb^{3+} ions were intercalated though excess MAs existed. Such Tb^{3+}-intercalated poly-PCDA exhibited completely reversible thermochromism, where almost all the carboxyl groups interacted with Tb^{3+} ions to form the nearly perfect structure. When the feeding molar ratio of PCDA, MA, and Tb^{3+} ion was 3:267:0.6, both Tb^{3+} ions and MAs were intercalated. There existed some defects in the imperfect MA-intercalated domains and at the domain boundaries. The MA/Tb^{3+}-intercalated poly-PCDA exhibits partially reversible thermochromism, where the backbones near the defects are hard to return the initial conformation, while the rest, those at nearly perfect organized domains, are still able to restore the initial conformation.

Key words: Polydiacetylene, Intercalation, Melamine, Tb^{3+} ion, Reversible thermochromism

I. INTRODUCTION

Polydiacetylene (PDA) is a family of intensively studied conjugated polymers because it has an intriguing supramolecular structure and stimuli-responsive property [1]. It has the π-conjugated backbone synthesized by the polymerization of diacetylene-containing monomer [1]. When subjected to the external stimuli, such as heat [2], pH [3, 4], solvent [5, 6], and mechanical stress [7, 8], PDA undergoes the color transition from blue (blue phase) to red (red phase). The color of PDA strongly depends on the planarity along the conjugated backbone [1]. The color transition is usually irreversible [1−8], which blocks the reusable application of PDA as the stimuli-responsive materials. Therefore, it is desirable to realize a reversible chromatic response under the external stimulus. In the past two decades, most of the research has focused on designing PDA materials to achieve reversible thermochromism. When the heat is applied to melt the crystalline layer of PDA, the mobility of side chains is enhanced, which

induces the torsion of the PDA backbone and the reduction of backbone planarity. It exhibits a blue-to-red thermochromic response [9, 10]. The reversible thermochromic response requires the backbone of PDA simultaneously to restore its original conformation and the color to return to its initial blue color once the temperature decreases [9, 10]. Generally, three strategies have been used to endow PDA with the reversible thermochromism effectively. They modified the side-chain terminal groups to enhance the interaction among the side chains [12], tethered the terminal groups of side chains onto the solid surface [13], and intercalated the guest components into the interlayer of PDA in order to tether the terminal groups of side chains to the intercalated layer [5−8, 13−15].

In these strategies, intercalation is a facile and versatile method. PDA monomer itself can self-assemble to the layered crystalline structure [1], which can serve as a host for intercalating guest components in the interlayer space. Take a typical PDA monomer for example, *i.e.* 10,12-pentacosdiynoic acid (PCDA). PCDA forms the lamellar bilayer crystalline structure [16−21]. The guest components can be successfully intercalated by coassembling PCDA with the guest components that are interactive with the carboxyl-terminal groups of PCDA. Finally, the guest-component intercalated stru-

*Authors to whom correspondence should be addressed. E-mail: huangxiayun@fudan.edu.cn, chendy@fudan.edu.cn, Tel.: +86-21-31245652

357

cture is obtained. A variety of guest components have been reported to be intercalated in PCDA successfully. For example, divalent transition metal ions (*i.e.*, Zn^{2+} ion) [16] and lanthanide metal ions (*i.e.*, Tb^{3+} ion and Dy^{3+} ion) [17, 18] could be intercalated into the interlayer of PCDA, where carboxyl-terminal groups of PCDA were tethered to the intercalated metal ion layer via coordination interaction. Guest organic amines, such as alkylamine [7] and melamine (MA) [19], could be accommodated inside the interlayer space of PCDA and formed a similar tethering structure through hydrogen bonding interaction. Poly(vinylpyrrolidone) (PVP) and poly(vinyl alcohol) (PVA) could also be intercalated into PCDA where carboxyl-terminal groups of PCDA were tethered to the intercalated polymer layer via hydrogen bonding interaction [20, 21]. In these intercalated structures, some of them could form the nearly perfect organized structure, where almost all the carboxyl-terminal groups of PCDA tethered to the intercalated layer. The corresponding poly-PCDA after polymerization mostly has a completely reversible thermochromic performance even though that of pure poly-PCDA is irreversible [7, 16−21]. Till now, the reported intercalated poly-PCDA structures have been made by only introducing a single component participant in the coassembly with PCDA. Some of them successfully achieved a completely reversible thermochromism. When two components, which are competitively interactive with carboxyl-terminal groups of PCDA, are chosen to coassemble with PCDA, the corresponding intercalation behavior and the thermochromic reversibility are interesting to learn but those have never been reported.

Herein, this work aims to understand the intercalation behavior and the corresponding thermochromic reversibility of the intercalated poly-PCDA when two components, Tb^{3+} ions and MAs, participate in the coassembly with PCDA. Both Tb^{3+} ion and MA can interact with carboxyl-terminal groups of PCDA via coordination interaction and hydrogen bonding interaction, respectively [17, 19]. Firstly, the PCDA ethanol solution was dropwise added to the MA aqueous solution to form the PCDA-MA coassemblies. Secondly, an additional amount of $TbCl_3$ aqueous solution was added to the suspension to prepare the PCDA-MA-Tb^{3+} coassemblies. During the annealing, the coassemblies reorganized themselves to a relative regular structure. In the annealed structure, only Tb^{3+} ions were intercalated when the feeding molar ratio of PCDA, MA, and Tb^{3+} ion was 3:267:1. Almost all the carboxyl groups of PCDA preferentially interacted with Tb^{3+} ions to form the nearly perfect Tb^{3+}-intercalated PCDA even though a large amount of MAs existed in the suspension. After photopolymerization, such Tb^{3+}-intercalated poly-PCDA exhibited completely reversible thermochromism. The suspension can return to the initial blue color during the 20th heating-cooling cycles. When the feeding molar ratio of PCDA, MA,

and Tb^{3+} ion was 3:267:0.6, both MAs and Tb^{3+} ions were intercalated. The MA/Tb^{3+}-intercalated PCDA had nearly perfect Tb^{3+}-intercalated domains, imperfect MA-intercalated domains, and defects located at the domain boundaries. After photopolymerization, these imperfect structures were preserved. Therefore, some of the poly-PCDA backbones near the defects are hard to have the synergic backbone rotation to return to the initial backbone conformation, which induces the irreversible formation of the red phase. The rest nearly perfect organized domains are still able to restore the initial conformation and form the blue phase. After the 1st heating-cooling cycle, the suspension has a mixture of blue phase and red phase and exhibits a purple color. During the 2nd−10th heating-cooling cycles, the nearly perfect organized domains are still able to restore the initial conformation, and the suspension reversibly switches between purple and red color.

II. EXPERIMENTS

A. Materials

10,12-Pentacosadiynoic acid (PCDA, $CH_3(CH_2)_{11}-$ $C{\equiv}C-C{\equiv}C-(CH_2)_8-COOH$), was purchased from GFS Chemicals, Inc. PCDA was purified step by step: (i) dissolving PCDA in absolute ethanol (200 Proof), (ii) filtering the PCDA solution through a 0.45 μm PTFE membrane to remove the polymerized impurity, (iii) drying the purified PCDA solution to powder by rotary evaporation. Melamine (MA) and terbium(III) chloride hexahydrate were purchased from Acros Organics and absolute ethanol (200 Proof) from Sinopham Chemical Reagent Co., Ltd., China, which were used as received without further purification.

B. Preparation of PCDA-MA-Tb^{3+} coassembly

8 mL of PCDA ethanol solution (1.25 mg/mL) was dropwise added to 100 mL of MA aqueous solution (3 mg/mL) at the feeding speed of 8 mL/h. Then, a certain amount of $TbCl_3$ aqueous solution (2 mmol/L) was added into the suspension at the feeding speed of 5 mL/h under mild stirring. The obtained suspension contains the PCDA-MA-Tb^{3+} coassembly. In this study, two different molar ratios of PCDA, MA, and Tb^{3+} ions were added, *i.e.*, PCDA:MA:Tb^{3+}=3:267:1 and 3:267:0.6.

C. Preparation of Tb^{3+}-intercalated poly-PCDA and MA/Tb^{3+}-intercalated poly-PCDA nanosheet

The PCDA-MA-Tb^{3+} coassembly suspensions were annealed at 68 °C for 6 h, obtaining the layered nanosheets. The annealed nanosheets were then dialyzed against water to remove free MA and Tb^{3+} ions.
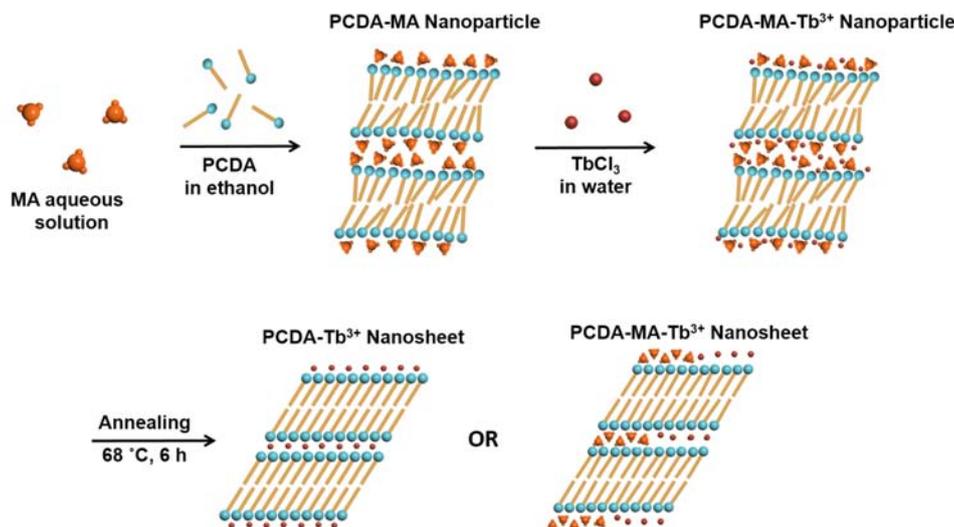
Scheme 1 Illustration of the preparation procedure of Tb^{3+}-intercalated PCDA and MA/Tb^{3+}-intercalated PCDA nanosheet. The PCDA-MA-Tb^{3+} coassemblies were firstly prepared. After annealed at 68 °C for 6 h, the coassemblies were reorganized to Tb^{3+}-intercalated or MA/Tb^{3+}-intercalated PCDA depending on the amount of PCDA, MA, and Tb^{3+} ion added. In the MA/Tb^{3+}-intercalated PCDA, there existed Tb^{3+}-intercalated and MA-intercalated domains.

After photopolymerization by exposing the nanosheet suspension under UV irradiation (25.5 W/cm^2, wavelength λ=254 nm) at room temperature for 5 min, the intercalated poly-PCDA nanosheet was obtained. When the feeding molar ratio of PCDA, MA, and Tb^{3+} ions was 3:267:1, Tb^{3+}-intercalated poly-PCDA nanosheets were obtained. When the feeding molar ratio of PCDA, MA, and Tb^{3+} ions was 3:267:0.6, MA/Tb^{3+}-intercalated poly-PCDA nanosheets were obtained.

D. Characterizations

The melting temperature of PCDA and PCDA-Tb^{3+} nanosheets were measured by the differential scanning calorimetry (DSC, TA Q2000) at the heating rate of 10 °C/min under the nitrogen flow. The morphologies of the nanosheets were characterized using the FEI Tecnai G20 TWIN transmission electron microscope (TEM) at the accelerating voltage of 200 kV. The hydrodynamic diameters and their distribution of the nanoparticles were examined by Zetasizer Nano ZS 90 (Malvern Instruments). The contents of C and N elements were measured by the elemental analyzer (Elementar, Vario EL). The content of Tb^{3+} ions was determined by using Inductively Coupled Plasma-Atomic Emission Spectrometry (ICP-AES, PerkinElmer, Optima 8000). The X-ray diffraction (XRD) spectra were measured using X'Pert PRO (X'Celerator diffractometer, operating at 40 kV, 40 mA, Cu Kα radiation, λ=0.15406 nm). UV-Vis spectra were measured by Shimadzu UV-2550 Spectrophotometer. The specimen was heated from 25 °C to 90 °C at the heating rate of

5 °C/min.

III. RESULTS AND DISCUSSION

A. Preparation of Tb^{3+}-intercalated poly-PCDA and MA/Tb^{3+}-intercalated poly-PCDA nanosheet

The PCDA-MA-Tb^{3+} coassemblies were prepared using two steps (Scheme 1). Firstly, PCDA-MA coassemblies were made by dropwise adding 8 mL of PCDA ethanol solution (1.25 mg/mL) to 100 mL of MA aqueous solution (3 mg/mL). Ethanol is a good solvent for PCDA, while water is a non-solvent for PCDA. Moreover, carboxyl groups of PCDA can interact with amine groups of MA via hydrogen bonding interaction [20]. In the mixture, insoluble PCDAs self-assemble with MAs and form PCDA-MA coassemblies. Secondly, an additional amount of TbCl$_3$ aqueous solution (2 mmol/L) was dropwise added into the PCDA-MA coassembly suspension till a certain feeding amount (PCDA:Tb^{3+}=3:1 or 5:1) was reached. Due to the coordination interaction between carboxyl groups of PCDA and Tb^{3+} ions [17], Tb^{3+} ions interacted with the carboxyl groups in the PCDA-MA coassemblies, obtaining the PCDA-MA-Tb^{3+} coassemblies.

Afterward, the obtained PCDA-MA-Tb^{3+} coassembly suspension was annealed at 68 °C for 6 h. During annealing, the coassemblies were expected to reorganize themselves to a relatively regular structure. The pure PCDA has a melting temperature of ∼63 °C (FIG. 1(a)). In our previous studies, nearly perfect Tb^{3+}-intercalated PCDA was obtained by annealing the PCDA-Tb^{3+} coassemblies at 68 °C for 6 h to melt
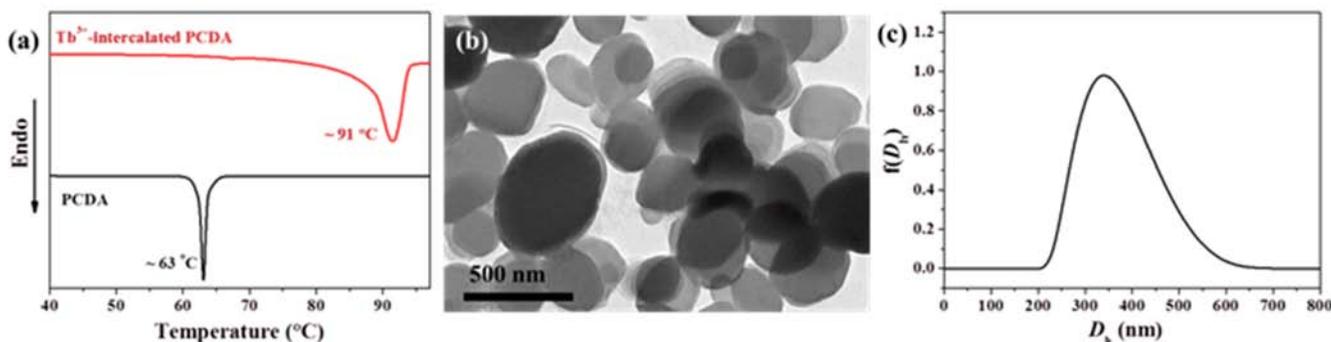
FIG. 1 (a) DSC curve of pure PCDA and Tb^{3+}-intercalated PCDA, (b) TEM image of Tb^{3+}-intercalated PCDA nanosheets, and (c) distribution of hydrodynamic diameter (D_h) of Tb^{3+}-intercalated PCDA nanosheets. The feeding molar ratio of PCDA, MA, and Tb^{3+} ion is 3:267:1.

the PCDA crystalline domain [17]. The resultant Tb^{3+}-intercalated PCDA has an increased melting temperature of ∼88 °C due to the reduced entropy change during the melting process by tethering the carboxyl groups of PCDA to the intercalated Tb^{3+} ion layer. Similarly, nearly perfect MA-intercalated PCDA obtained by being annealed at 65 °C for 6 h also has an increased melting temperature (83 °C) [22].

PCDA, MA, and Tb^{3+} ion at the molar ratio of 3:267:1 were added to prepare the PCDA-MA-Tb^{3+} coassembly suspension, which was then annealed at 68 °C for 6 h. The annealed coassemblies have a relatively sharp melting peak and an increased melting temperature at 91 °C (FIG. 1(a)), which is close to the melting temperatures of nearly perfect Tb^{3+}-intercalated PCDA and nearly perfect MA-intercalated PCDA [17, 22]. Therefore, annealing at 68 °C for 6 h is a proper annealing condition to obtain the nearly perfect intercalation structure. In the intercalated PCDA, the intercalated components are homogeneously distributed. The intercalated PCDA has the nanosheet structure with an average hydrodynamic diameter (D_h) of 350 nm and a polydispersity index (PDI) of 0.053 (FIG. 1 (b) and (c)).

Since both Tb^{3+} ions and MAs can interact with carboxyl groups of PCDA [17, 19, 22], the intercalated PCDA might have MAs to be intercalated, Tb^{3+} ions to be intercalated, or both MAs and Tb^{3+} ions to be intercalated. The elemental analysis result shows that there is not any MA existing in the intercalated PCDA (Table S1 in supplementary materials). However, it has Tb^{3+} ions to be intercalated as confirmed by ICP-AES (Table S1 in supplementary materials). Therefore, it is named as Tb^{3+}-intercalated PCDA nanosheet since only Tb^{3+} ions are intercalated and it has the nanosheet structure.

In our previous study of Tb^{3+}-intercalated PCDA [17], when the PCDAs and Tb^{3+} ions were added at the molar ratio of 3:1, after annealing, almost all the carboxyl groups of PCDA behaved as the bidentate ligands to be tethered to the intercalated Tb^{3+} ion layer,

and therefore provided the intercalated PCDA. In the case when PCDA, MA, and Tb^{3+} ion were added at the molar ratio of 3:267:1, the resultant intercalated PCDA after annealing only has the Tb^{3+} ions intercalated. Therefore, the coordination interaction between the Tb^{3+} ion and the carboxyl group of PCDA is stronger than the hydrogen bonding interaction between the amine group of MA and the carboxyl group of PCDA. The carboxyl groups of PCDA preferentially interact with Tb^{3+} ions even though a large amount of MAs exist in the suspension. In the Tb^{3+}-intercalated PCDA nanosheet, the molar ratio of PCDA and Tb^{3+} ion is measured to be approximately 3:1 by detecting the concentrations of C element and Tb^{3+} ion in the nanosheet. Almost all the carboxyl groups of PCDA are involved in the interaction with the intercalated Tb^{3+} ion layer via bidentate chelation. Since almost all the carboxyl groups of PCDA engage in the interaction with Tb^{3+} ions, there do not remain any carboxyl groups to interact with MAs in the suspension. The Tb^{3+}-intercalated PCDA nanosheet has the lamellar structure with the d-spacing of 5.40 nm (FIG. 2(a)), which is similar to the lamellar structure of Tb^{3+}-intercalated PCDA nanosheets (d-spacing of 5.40 nm) obtained by annealing PCDA-Tb^{3+} coassemblies [17]. Although both MA and Tb^{3+} ion in the suspension can coassemble with PCDA, the existed MAs in the suspension do not distinguishably influence the formation of the Tb^{3+}-intercalated lamellar structure.

From the above study, we learn that carboxyl groups of PCDA preferentially interact with Tb^{3+} ions even when MAs existed in the suspension. When there are enough Tb^{3+} ions in the suspension to interact with the carboxyl groups of PCDA, MAs cannot be intercalated. When less amount of Tb^{3+} ions is added, only some of the carboxyl groups of PCDA interact with Tb^{3+} ions via bidentate chelation. The rest carboxyl groups that do not interact with Tb^{3+} ions might interact with the amine groups of MAs via hydrogen bonding interaction. Therefore, we investigate the intercalation behavior of this system. In specific, the same amount of PCDA and
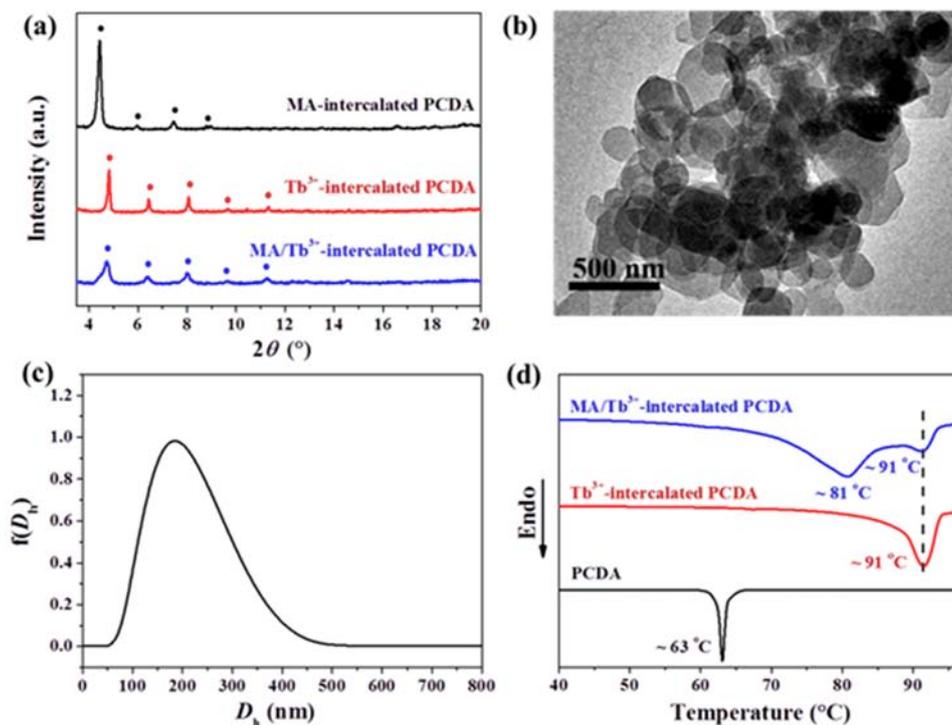
FIG. 2 (a) XRD patterns of MA-intercalated PCDA, Tb^{3+}-intercalated PCDA and MA/Tb^{3+}-intercalated PCDA, (b) TEM image of MA/Tb^{3+}-intercalated PCDA nanosheets, (c) distribution of hydrodynamic diameter (D_h) of MA/Tb^{3+}-intercalated PCDA nanosheet, and (d) DSC curve of PCDA, Tb^{3+}-intercalated PCDA and MA/Tb^{3+}-intercalated PCDA. The feeding molar ratio of PCDA, MA, and Tb^{3+} ion is 3:267:0.6.

MA were added to prepare the PCDA-MA coassemblies. Then, less amount of Tb^{3+} was added to prepare the PCDA-MA-Tb^{3+} coassemblies. The molar ratio of PCDA, MA, and Tb^{3+} ion added to the suspension is 3:267:0.6. After annealing at 68 °C for 6 h, both Tb^{3+} ions and MAs have been intercalated confirmed by the elemental analysis and ICP-AES (Table S1 in supplementary materials). MA/Tb^{3+}-intercalated PCDA has the nanosheet structure with an average D_h of 200 nm and PDI of 0.032 (FIG. 2 (b) and (c)). The obtained PCDA is therefore named as MA/Tb^{3+}-intercalated PCDA nanosheet.

When both Tb^{3+} ions and MAs were intercalated, they might be molecularly homogenously distributed in the interlayer of PCDA or form the Tb^{3+}-intercalated and MA-intercalated domains distributed in the same interlayer or separately in the different interlayers of PCDA. From the XRD pattern, only a single d-spacing (5.60 nm) was observed in the MA/Tb^{3+}-intercalated PCDA, which was larger than that of Tb^{3+}-intercalated PCDA (d-spacing of 5.40 nm) and smaller than that of MA-intercalated PCDA (d-spacing of 5.96 nm) (FIG. 2(a)). Therefore, the circumstance that the Tb^{3+}-intercalated and the MA-intercalated domains locate separately in the different interlayer of PCDA does not exist since the d-spacing of Tb^{3+}-intercalated and the MA-intercalated domains are not observed. However, there still exist two possible circum-

stances, in which Tb^{3+} ions and MAs are molecularly homogenously distributed in the interlayer of PCDA or homogeneously distributed in the interlayer of PCDA in the form of Tb^{3+}-intercalated and the MA-intercalated domains.

As mentioned, the intercalated PCDA can have an increased melting temperature because the carboxyl groups of PCDA were tethered to the intercalated layer, which reduced the entropy change during the melting process. When Tb^{3+} ions and MAs are molecularly homogenously distributed in the interlayer of PCDA, the carboxyl groups of PCDA can be equivalent to be tethered to the intercalated layer uniformly, and the obtained PCDA should have a single melting peak. However, the DSC curve of the MA/Tb^{3+}-intercalated PCDA nanosheet exhibits two melting peaks at ∼81 and ∼91 °C (FIG. 2(d)), indicating that Tb^{3+} ions and MAs are homogeneously distributed in the interlayer of PCDA in the form of Tb^{3+}-intercalated and the MA-intercalated domains instead of the molecularly homogeneous distribution.

The molar ratio of PCDA to Tb^{3+} ion in the MA/Tb^{3+}-intercalated PCDA was measured to be approximately 5:1 (Table S1 in supplementary materials), which was close to the molar ratio of PCDA and Tb^{3+} ion added in the suspension. Thus, almost all the Tb^{3+} ions in the suspension participate in the coassembly. Moreover, annealing at 68 °C for 6 h has proved
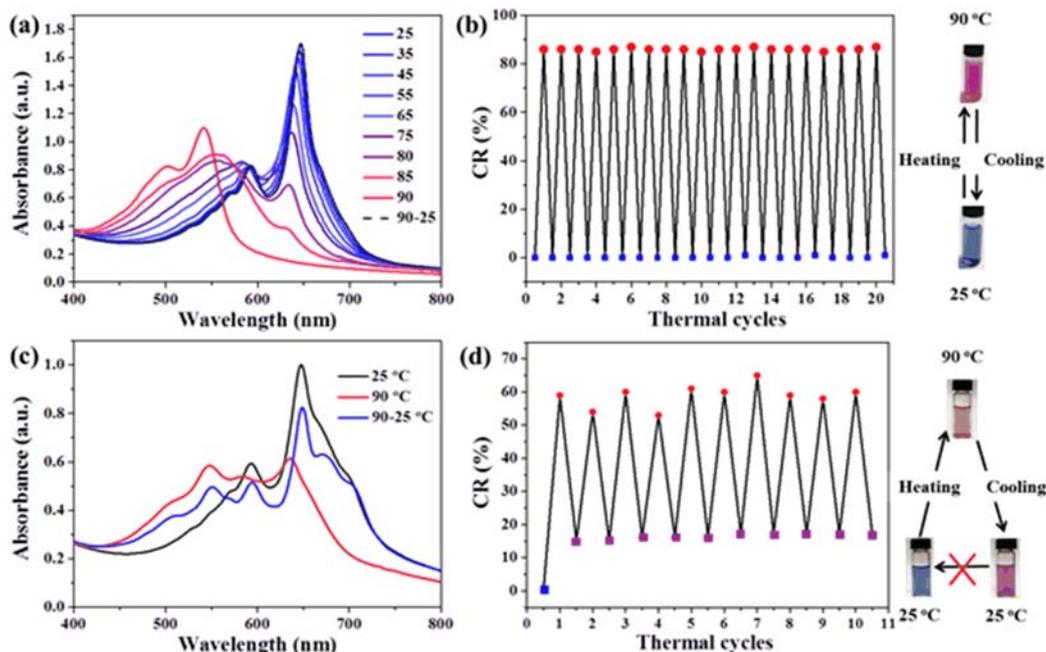
FIG. 3 (a) UV-Vis spectra of Tb^{3+}-intercalated poly-PCDA nanosheet suspension at different temperatures. The abrupt shift of λ_{max} to ca. 550 nm occurred at 80 °C. The dashed line represents the spectrum of the suspension after cooling to 25 °C from 90 °C, indicating the complete reversibility of nanosheet suspension. (b) Colorimetric response (CR) of Tb^{3+}-intercalated poly-PCDA nanosheet suspension demonstrated its completely reversible thermochromism. The red nanosheet suspension at 90 °C could fully return to the initial blue color when it was cooled to 25 °C during the 20th heating-cooling cycles. (c) UV-Vis spectra of MA/Tb^{3+}-intercalated poly-PCDA nanosheet suspension during the 1st heating-cooling cycle between 25 °C and 90 °C. (d) CR of nanosheet suspension demonstrated its partial thermochromic reversibility. The red nanosheet suspension at 90 °C yielded to purple color when it was cooled to 25 °C at the 1st heating-cooling cycle. During the 2nd−10th heating-cooling cycles, the suspension alternately switched between purple and red color.

to be a proper annealing condition for obtaining the nearly perfect Tb^{3+}-intercalated structure. The Tb^{3+}-intercalated domain has the melting temperature of ∼91 °C, which is the same as that of Tb^{3+}-intercalated PCDA annealed at the same condition. The carboxyl groups of PCDA preferentially interact with Tb^{3+} ions via bidentate chelation (PCDA:Tb^{3+}=3:1). Therefore, there are about three-fifths of the carboxyl groups involved in the interaction with Tb^{3+} ions. The rest two-fifths of carboxyl groups that do not interact with Tb^{3+} ions can interact with MAs. As reported in our previous work [19], the nearly perfect MA-intercalated PCDA had an ideal double-layer MA-intercalated structure, in which the molar ratio of PDCA to MA was about 2:1. In this work, the molar ratio of PCDA to MA in the MA/Tb^{3+}-intercalated PCDA is estimated to be about 8:1 (Table S1 in supplementary materials). Considering about two-fifths of the carboxyl groups interact with MA, the molar ratio of the PCDA involved in the interaction with MA to MA in the intercalated PCDA is 3.2:1, which is larger than the ratio in the ideal double-layer MA-intercalated structure. There are not enough MAs to be intercalated to achieve the ideal double-layer structure. Therefore, the obtained MA-intercalated domain has an imperfect intercalation

structure. Except for lots of defects existing in the imperfect MA-intercalated domains, there are also defects at the domain boundaries. They all contribute to the lower broad melting peak at ∼81 °C.

At this point, we have successfully prepared the Tb^{3+}-intercalated PCDA and MA/Tb^{3+}-intercalated PCDA nanosheets. The intercalated nanosheets were then photopolymerized to form the ene-yne backbone, adopting the side chains with an all-*trans* conformation [17−22]. Both Tb^{3+}-intercalated poly-PCDA and MA/Tb^{3+}-intercalated poly-PCDA nanosheet suspension display a blue color and have two absorption peaks at ca. 590 and 645 nm (FIG. 3).

B. Thermochromic reversibility of Tb^{3+}-intercalated poly-PCDA and MA/Tb^{3+}-intercalated poly-PCDA nanosheet

As discussed above, Tb^{3+}-intercalated PCDA has a nearly perfect organized structure, while MA/Tb^{3+}-intercalated PCDA has lots of defects in the imperfect MA-intercalated domains and at the domain boundaries. After photopolymerization, these perfect and imperfect organized structures were preserved and might have different performance in thermochromic re-

versibility. Therefore, the thermochromic reversibility of Tb^{3+}-intercalated poly-PCDA and MA/Tb^{3+}-intercalated poly-PCDA were investigated (FIG. 3).

At 25 °C, Tb^{3+}-intercalated poly-PCDA nanosheet suspension has a blue color and exhibits a maximum absorption peak at ca. 645 nm, which is the characteristic absorption peak of the blue phase. Upon heating, the intensity of the absorption peak at ca. 645 nm gradually decreased, and the maximum absorption peak continuously shifted to the lower wavelength. The abrupt shift of $\lambda_{\max}$ to ca. 550 nm occurred at 80 °C. With continuous raising the temperature to 90 °C, the Tb^{3+}-intercalated poly-PCDA nanosheet suspension became red and shifted to the characteristic absorption peak of the red phase at ca. 545 nm. Afterward, the suspension was cooled to 25 °C. It returned to the initial blue color with the UV-Vis spectrum being almost overlapped with that before the heating-cooling cycle (black dash line in FIG. 3(a)). The performance of thermochromic reversibility from the blue phase to the red phase can be evaluated by the colorimetric response (CR), CR$=(B_0-B_{\text{temperature}})/B_0\times100\%$ and $B_{\text{temperature}}=A_{645}/(A_{645}+A_{545})$, where B_0 is the initial value and A_{545} and A_{645} are the absorbances of the red phase and blue phase of poly-PCDA at the corresponding wavelength, respectively [17]. The Tb^{3+}-intercalated poly-PCDA nanosheet suspension was repeatedly heated to 90 °C and cooled to 25 °C for 20 cycles. As shown in FIG. 3(b), the color of the suspension alternately switched between blue and red during the heating-cooling cycles. The CR switching could be repeated for 20th heating-cooling cycles, indicating that Tb^{3+}-intercalated poly-PCDA nanosheet suspension has completely reversible thermochromism.

The nearly perfect organized intercalated structure is a critical factor to achieve its excellent reversible thermochromic performance [9, 10]. When the heat was applied to melt the alkyl crystalline layers of Tb^{3+}-intercalated poly-PCDA nanosheet, the increased mobility of poly-PCDA side chains led to the torsion of backbone and thus the planarity of backbone was reduced. The nanosheet suspension displayed a red color. At this moment, the carboxyl-terminal groups of poly-PCDA were still tethered to the intercalated Tb^{3+} ion layers. Once the nanosheet suspension was cooled to 25 °C, the crystallization of the alkyl side chains forced the backbone to restore its original blue phase conformation and realized the completely reversible thermochromism.

In comparison, MA/Tb^{3+}-intercalated poly-PCDA has lots of defects existing in the imperfect MA-intercalated domains and at the domain boundaries. At 25 °C, the suspension also has a blue color and exhibits the characteristic blue phase absorption peak at ca. 645 nm (FIG. 3(c)). When heated to 90 °C, the MA/Tb^{3+}-intercalated poly-PCDA nanosheet suspension becomes red and shifts to the characteristic red phase absorption peak at ca. 545 nm. However, when

cooled to 25 °C, the suspension returns to the purple color instead of the initial blue color (blue line in FIG. 3(c)), exhibiting the partial thermochromic reversibility. The MA/Tb^{3+}-intercalated poly-PCDA nanosheet suspension in purple color is the mixtures of red phase and blue phase. The backbone near the defect is hard to have the synergic backbone rotation to return the initial conformation, which induces the irreversible formation of the red phase. The rest nearly perfect organized intercalated domains are still able to restore the initial conformation and form the blue phase. During the 2nd−10th heating-cooling cycle from 25 °C to 90 °C, the color of the suspension alternately switchs between purple and red color. This transition from purple to red is entirely reversible as confirmed by CR values (FIG. 3(d)), indicating the nearly perfect organized intercalated domains exhibit the completely thermochromic reversibility.

IV. CONCLUSION

The MA/Tb^{3+}-intercalated poly-PCDA nanosheets were successfully fabricated when PCDA, MA, and Tb^{3+} were added at the feed molar ratio of 3:267:0.6. In comparison, when the feeding molar ratio of PCDA, MA, and Tb^{3+} ion was 3:267:1, only Tb^{3+} ions were intercalated in the poly-PCDA nanosheets even though there existed excess MAs in the suspension. During annealing, the carboxyl groups of PCDA preferentially interacted with Tb^{3+} ions and formed the nearly perfect organized structure. When there are enough Tb^{3+} ions to interact with almost all the carboxyl groups of PCDA, MAs cannot be intercalated. The obtained Tb^{3+}-intercalated poly-PCDA has the nearly perfect organized structure and exhibits completely reversible thermochromism. When less amount of Tb^{3+} is added, some of the carboxyl groups of PCDA interact with Tb^{3+} ions while the rest interact with MAs. The obtained MA/Tb^{3+}-intercalated poly-PCDA has some defects in the imperfect MA-intercalated domains and at the domain boundaries. It exhibits partially reversible thermochromism, where the backbones near the defects are hard to return to the initial conformation, while the rest, those at nearly perfect organized domains, are still able to restore the initial conformation.

Supplementary materials: Elemental analyses and ICP-AES results of Tb^{3+}-intercalated PCDA and MA/Tb^{3+}-intercalated PCDA nanosheet are available.

V. ACKNOWLEDGMENTS

[1] K. S. Mali, N. Pearce, S. De Feyter, and N. R. Champness, Chem. Soc. Rev. **46**, 2520 (2017).

[2] J. M. Kim, J. S. Lee, H. Choi, D. Sohn, and D. J. Ahn, Macromolecules **38**, 9366 (2005).

[3] U. Jonas, K. Shah, S. Norvez, and D. H. Charych, J. Am. Chem. Soc. **121**, 4580 (1999).

[4] Z. Yuan and T. W. Hanks, Polymer **49**, 5023 (2008).

[5] S. Wu, L. Pan, Y. J. Huang, N. Yang, and Q. J. Zhang, Soft Matter **14**, 6929 (2018).

[6] C. Khanantonga, N. Charoenthaia, S. Wacharasindhu, M. Sukwattanasinitt, N. Traiphol, and R. Traiphol, J. Ind. Eng. Chem. **58**, 258 (2018).

[7] Y. Ishijima, H. Imai, and Y. Oaki, Chem. **3**, 1 (2017).

[8] H. Terada, H. Imai, and Y. Oaki, Adv. Mater. **30**, 1801121 (2018).

[9] X. Q. Chen, G. D. Zhou, X. J. Peng, and J. Yoon, Chem. Soc. Rev. **41**, 4610 (2012).

[10] X. M. Sun, T. Chen, S. Q. Huang, L. Li, and H. S. Peng, Chem. Soc. Rev. **39**, 4244 (2010).

[11] S. Wacharasindhu, S. Montha, J Boonyiseng, A Poti-satityuenyong, C. Phollookin, G. Tumcharern, and M. Sukwattanasinitt, Macromolecules **43**, 716 (2010).

[12] T. V. Oliveira, N. F. F. Soares, J. S. R. Coimbra, N. J. Andrade, L. G. Moura, E. A. A. Medeiros, and H. S. Medeiros, Sens. Actuators B: Chem. **221**, 653 (2015).

[13] M. Takeuchi, H. Imai, and Y. Oaki, ACS Appl. Mater. Interfaces **9**, 16457 (2017).

[14] M. Takeuchi, H. Imai, and Y. Oaki, J. Mater. Chem. C **5**, 8250 (2017).

[15] S. Chae, J. P. Lee, and J. M. Kim, Adv. Funct. Mater. **26**, 1769 (2016).

[16] M. Okaniwa, Y. Oaki, and H. Imai, Adv. Funct. Mater. **26**, 3463 (2016).

[17] Y. S. Yao, K. Y. Fu, X. Y. Huang, and D. Y. Chen, Chin. J. Chem. **35**, 1678 (2017).

[18] K. Y. Fu and D. Y. Chen, Chin. J. Chem. Phys. **27**, 465 (2014).

[19] J. Guo, K. Y. Fu, Z. B. Zhang, L. Y. Yang, Y. C. Huang, C. I. Huang, L. Zhu, and D. Y. Chen, Polymer **105**, 440 (2016).

[20] Y. Gu, W. Q. Cao, L. Zhu, D. Y. Chen, and M. Jiang, Macromolecules **41**, 2299 (2008).

[21] J. Guo, L. Zhu, M. Jiang, and D. Y. Chen, Langmuir **27**, 6651 (2011).

[22] K. Y. Fu, *Master Thesis*, Shanghai: Fudan University, No.052044007 (2014).